THE JOURNAL OF PHYSICAL CHEMISTRY A

Article

pubs.acs.org/JPCA

Extended Polarization in Third-Order SCC-DFTB from Chemical-Potential Equalization

Steve Kaminski,[†] Timothy J. Giese,[‡] Michael Gaus,[§] Darrin M. York,*[,‡] and Marcus Elstner*[,†]

[†]Institut für physikalische Chemie, Karlsruher Institut für Technologie, Kaiserstrasse 12, D-76131 Karlsruhe, Germany

[‡]BioMaPS Institute and Department of Chemistry and Chemical Biology, Rutgers University, Piscataway, New Jersey 08854-8087, United States

[§]Department of Chemistry and Theoretical Chemistry Institute, University of Wisconsin, Madison, 1101 University Avenue, Madison, Wisconsin 53706, United States

Supporting Information

ABSTRACT: In this work, we augment the approximate density functional method SCC-DFTB (DFTB3) with the chemical-potential equalization (CPE) approach in order to improve the performance for molecular electronic polarizabilities. The CPE method, originally implemented for the NDDO type of methods by Giese and York, has been shown to significantly emend minimal basis methods with respect to the response properties and has been applied to SCC-DFTB recently. CPE allows this inherent limitation of minimal basis methods to be overcome by supplying an additional response density. The systematic underestimation is thereby corrected quantitatively without the need to extend the atomic orbital basis (i.e., without increasing the overall computational cost significantly). The dependency of polarizability as a function of the molecular charge state, especially, was significantly improved from the CPE extension of DFTB3. The empirical parameters introduced by the CPE approach were optimized for 172 organic molecules in order to match the results from density functional theory methods using large basis sets. However, the first-order derivatives of molecular polarizabilities (e.g., required to compute Raman activities) are not improved by the current CPE implementation (i.e., Raman spectra are not improved).

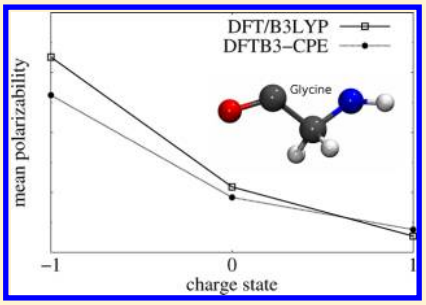

INTRODUCTION

Semiempirical (SE) theory has made huge progress through the decades.[1−5] Starting from successful models of the early days like MNDO, AM1, and PM3,[6−8] many improvements in the formalism and parametrization have led to a new generation of SE methods,[9−13,36] all derived from the Hartree−Fock (HF) theory, yet, treating the important effects of electron correlation implicitly. A second route to SE methods starts with density functional theory[19,20] (DFT), introducing several approximations which result in an increase by 2−3 orders of magnitude with respect to (wrt) the DFT methods with medium-sized basis sets.

The approximations are threefold:

(i) One approximation is the expansion of the DFT total energy around a suitably chosen reference density in first[23] (DFTB), second[24] (DFTB2), and third order[30,31,35] (DFTB3). While the second-order terms are crucial for polar molecules, the third-order expansion becomes indispensable for charged molecular species. In DFTB, this expansion is truncated after the monopole term at every order. In second order, this allows for the inclusion of the effect of charge transfer between atoms in the energy expression and in third order for the change of atomic hardness with charge state. However, the nonspherical charge redistribution around the atoms is neglected. This expansion has been analyzed in more detail recently by York and co-workers.[33]

(ii) The second is the neglect and approximation of interaction integrals. In particular, this concerns the neglect of two-center integrals for the diagonal terms and three-center integrals for the off-diagonal contributions.[23] Further, the DFT "double counting" contributions are grouped into a pairwise potential, which is determined by comparison with DFT calculations[23] or fitted to the empirical data.[32]

(iii) The third approximation is the use of a minimal basis, which is part of the computational efficiency since it significantly reduces the size of the eigenvalue problem to be solved. However, this approximation is also the core of the problem when it comes to the calculations of response properties.

Among the multitude of molecular properties to which SE models were applied for evaluation, molecular electronic polarizability remains a challenging one since SE models mostly work with a minimal molecular-orbital basis to gain efficiency. It has been shown,[28] however, that the size of the ao-basis is a crucial aspect for the accuracy of polarization, which is underestimated by an average of 25% from SE methods[43] compared to experimental results. To overcome this limitation without increasing the ao-basis itself, which would lower the

Received: June 25, 2012
Revised: August 13, 2012
Published: August 15, 2012

dx.doi.org/10.1021/jp306239c | J. Phys. Chem. A 2012, 116, 9131−9141

efficiency of the SE methods significantly, empirical models were proposed (e.g., for neglect of differential overlap (NDDO)-based SE methods)[16−5] that originated from perturbation theory.[14−16] Another approach which has been shown to be promising is the chemical-potential equalization (CPE) method, created by Sanderson[25] as an electronegativity-equalization approach, which was later modified and improved.[26,27] In the framework of CPE extended MNDO[38] and second-order SCC-DFT[33] (DFTB2), Giese and York were able to accurately reproduce polarizabilities compared to DFT with a large ao-basis. Concerning SCC-DFTB, the accuracy is limited not only by the minimal ao-basis approach but also by the monopole basis representation of charge density fluctuations in second order.[31]

In the present work, we discuss the implementation, parametrization, and performance of the CPE extended third-order SCC-DFTB (DFTB3) method for polarizability calculations. Although the third-order expansion denotes a clear step forward over the DFTB2 formalism,[35] DFTB3 suffers from the same basic limitations as DFTB2 for polarizability calculations (i.e., the minimal basis and the monopole representation of charge fluctuations). For the treatment of phosphorus-containing molecules (e.g., which cannot be properly described by DFTB2), DFTB3 is an important step forward. In this respect, a DFTB3/CPE approach would be especially beneficial for studies of DNA, in which the polarization effect of the highly negatively charged phosphate backbone would be significantly underestimated by standard DFTB3.

As a step forward, we will also evaluate in this work the potential of the current CPE formalism to accurately reproduce Raman intensities, since they depend on first-order polarizability derivatives wrt normal mode vibrations. Concerning Raman intensities, we take a closer look at the polarizability tensor as a whole, while most of the previous studies[17,18,33,36,38] focused just on the mean polarizability (i.e., the average of the tensor's diagonal elements).

THEORETICAL APPROACH

Theory of Third-Order SCC-DFTB. The extension of the DFTB2 approach to the third order (DFTB3) has been introduced recently[31,35] and will be briefly summarized below. The starting point to derive the DFTB3 total energy is the energy expression of the Kohn−Sham DFT.[20] Instead of finding the electron density, $\rho(\mathbf{r})$, that minimizes the energy, a reference density, ρ^0, is assumed which is perturbed by some density fluctuation, $\rho(\mathbf{r}) = \rho^0(\mathbf{r}) + \delta\rho(\mathbf{r})$. The exchange-correlation energy functional is then expanded in a Taylor series up to the third order, and the total energy can be written as

$$\begin{aligned} E^{\mathrm{dftb3}}[\rho^0 + \delta\rho] = {} & \sum_i n_i \langle\psi_i|\hat{H}[\rho^0]|\psi_i\rangle \\ & - \frac{1}{2}\iint \frac{\rho^0(\mathbf{r})\,\rho^0(\mathbf{r}')}{|\mathbf{r}-\mathbf{r}'|}\,\mathrm{d}\mathbf{r}\,\mathrm{d}\mathbf{r}' - \int V^{\mathrm{xc}}[\rho^0]\rho^0(\mathbf{r})\,\mathrm{d}\mathbf{r} \\ & + E^{\mathrm{xc}}[\rho^0] + E^{\mathrm{nn}} \\ & + \frac{1}{2}\iint \left(\frac{1}{|\mathbf{r}-\mathbf{r}'|} + \left.\frac{\delta^2 E^{\mathrm{xc}}[\rho]}{\delta\rho(\mathbf{r})\,\delta\rho(\mathbf{r}')}\right|_{\rho^0}\right)\delta\rho(\mathbf{r}) \\ & \delta\rho(\mathbf{r}')\,\mathrm{d}\mathbf{r}\,\mathrm{d}\mathbf{r}' + \frac{1}{6}\iiint \left.\frac{\delta^3 E^{\mathrm{xc}}[\rho]}{\delta\rho(\mathbf{r})\,\delta\rho(\mathbf{r}')\,\delta\rho(\mathbf{r}'')}\right|_{\rho^0} \\ & \delta\rho(\mathbf{r})\,\delta\rho(\mathbf{r}')\,\delta\rho(\mathbf{r}'')\,\mathrm{d}\mathbf{r}\,\mathrm{d}\mathbf{r}'\,\mathrm{d}\mathbf{r}'' \end{aligned} \tag{1}$$

Several approximations follow: first, the Kohn−Sham orbitals, ψ_i, are represented in a minimal basis of pseudoatomic orbitals, $\psi_i = \sum_\mu c_{\mu i}\phi_\mu$. The diagonal elements of the resulting Hamiltonian matrix $\mathbf{H}^0_{\mu\nu}$ (first term of eq 1) are chosen to be atomic DFT eigenvalues evaluated with the PBE[22] exchange-correlation functional, and the off-diagonal elements are calculated in a two-center approximation.[34] Second, the double counting terms (second to fifth terms of eq 1), the exchange-correlation energy at the reference density, $E^{\mathrm{xc}}[\rho^0]$, and the nucleus−nucleus interaction, E^{nn}, are approximated as two-center pair potentials V^{rep}_{ab}. Third, the charge density fluctuation $\delta\rho$ is written as a superposition of atomic contributions $\delta\rho = \sum_a \delta\rho_a$, where the atomic contributions are approximated as spherical charge distributions by a simple Slater function with the magnitude of the Mulliken charge, q_a, of that atom centered around coordinate $\mathbf{R}_a$:

$$\delta\rho_a \approx q_a \frac{\tau_a^3}{8\pi} \mathrm{e}^{-\tau_a|\mathbf{r}-\mathbf{R}_a|} \tag{2}$$

Using this approximation, the Coulomb interaction of the second-order term wrt $\delta\rho$ can be expressed analytically and is abbreviated as γ_{ab} below. The exponent τ_a is chosen such that the onsite value of the γ-function properly describes the atomic chemical hardness (or alternatively the Hubbard parameter as calculated from DFT) and, thus, implicitly takes into account the exchange-correlation contribution to the second-order term. For improving this interpolation between long-range Coulomb interactions and the onsite term, further refinements of the γ-function have been applied.[35] For the third-order term, a Γ-function is defined which results in the derivative of the γ-function wrt charge, by introducing the Hubbard derivative parameter which expresses the change of the Hubbard parameter wrt the charge state of that atom in a linear way. It has been shown that a third-order term from a more rigorous density-functional expansion does not contribute significantly to the accuracy of the method.[33] In that way, the third-order terms within SCC-DFTB can be seen as a rather robust way to introduce the charge dependence, capturing some deficiencies of problematic approximations within the second-order formalism, namely, the small size of the pseudoatomic orbital basis and the very simplified density fluctuation scheme. With all these approximations the SCC-DFTB total energy in the third order is given by

$$\begin{aligned} E^{\mathrm{dftb3}} = {} & \sum_{iab}\sum_{\mu\in a}\sum_{\nu\in b} n_i c_{\mu i} c_{\nu i} H^0_{\mu\nu} \\ & + \frac{1}{2}\sum_{ab} q_a q_b \gamma_{ab} + \frac{1}{3}\sum_{ab} {q_a}^2 q_b \Gamma_{ab} + \frac{1}{2}\sum_{ab} V^{\mathrm{rep}}_{ab} \end{aligned} \tag{3}$$

The derivative of this expression wrt the molecular orbital coefficients leads to the corresponding Kohn−Sham equations

$$\sum_\nu c_{\nu i}(H_{\mu\nu} - \varepsilon_i S_{\mu\nu}) = 0 \quad \text{with } \nu \in b \text{ and } \forall\, a, \mu \in a \tag{4}$$

$$\begin{aligned} H_{\mu\nu} = {} & H^0_{\mu\nu} + S_{\mu\nu}\sum_c q_c\left(\frac{1}{2}(\gamma_{ac} + \gamma_{bc}) + \frac{1}{3}(q_a\Gamma_{ac} + q_b\Gamma_{bc})\right. \\ & \left. + \frac{q_c}{6}(\Gamma_{ca} + \Gamma_{cb})\right) \end{aligned} \tag{5}$$

dx.doi.org/10.1021/jp306239c | J. Phys. Chem. A 2012, 116, 9131−9141

where $S_{\mu\nu}$ is the overlap matrix. The Hamilton matrix elements depend on the Mulliken charges which in turn depend on the molecular orbital coefficients, $c_{\mu i}$; thus, these equations have to be solved self-consistently.

For DFTB3, molecular electronic polarizabilities were evaluated via the finite electric-field approach as

$$\alpha_{ij} = \left(\frac{\partial \mu_i}{\partial F_j}\right) i, j = x, y, z \tag{6}$$

where F_j is the Cartesian component of an externally applied electric field. To capture the effect of the field perturbing the system, an extra term[29] is added to the DFTB3 energy expression, describing the interaction of the field with the induced Mulliken charges of the system, as

$$E^{\text{field}} = E - \sum_A q_A \sum_{j=1}^{3} F_j x_{jA} \tag{7}$$

Here, x_{jA} denotes the Cartesian coordinate of atom A in direction j. The charge self-consistent Hamiltonian becomes

$$\mathbf{H}_{\mu\nu}^{\text{field}} = \mathbf{H}_{\mu\nu} - \frac{1}{2} S_{\mu\nu} \sum_{j=1}^{3} D_j x_{jA} \tag{8}$$

The CPE Approach and Its Implementation into DFTB3. In the framework of extending the DFTB3 by the chemical-potential equalization method, we follow the ideas of York and Giese.[36−38] The total energy of the system can be written as

$$E_{\text{tot}}[\rho] = E^{\text{dftb3}}[\rho] + E_{\text{cpe}}[\rho] \tag{9}$$

where $E_{\text{dftb3}}[\rho]$ is the DFTB3 energy and $E_{\text{cpe}}[\rho]$ is a self-consistent CPE response correction. CPE uses the DFTB3 charge density as a reference in a second-order Taylor series expansion of an approximate density functional. To derive the expression for $E_{\text{cpe}}[\rho]$, we define the density functional generically as

$$E[\rho] = \int \nu(\mathbf{r})\, \rho(\mathbf{r})\, \mathrm{d}^3 r + F[\rho] \tag{10}$$

and the Taylor expansion becomes

$$E[\rho^{\text{ref}} + \delta\rho^{\text{cpe}}] - E[\rho^{\text{ref}}] = \int \left[\frac{\delta E[\rho]}{\delta \rho(\mathbf{r})}\right]_{\rho=\rho^{\text{ref}}} \delta\rho^{\text{cpe}}(\mathbf{r})\, d^3 r + \frac{1}{2} \iint \left[\frac{\delta^2 F[\rho]}{\delta\rho(\mathbf{r})\, \delta\rho(\mathbf{r}')}\right]_{\rho=\rho^{\text{ref}}} \delta\rho^{\text{cpe}}(\mathbf{r})\, \delta\rho^{\text{cpe}}(\mathbf{r}')\, d^3 r\, d^3 r' \tag{11}$$

In the framework of the current CPE implementation, the response density $\delta\rho^{\text{cpe}}$ is expressed in a basis of functions, φ^{cpe}, as

$$\delta\rho^{\text{cpe}}(\mathbf{r}) = \sum_i c_i \varphi_i^{\text{cpe}}(\mathbf{r}) \tag{12}$$

where the response coefficients, c_i, are unknown and have to be evaluated through a variational approach. Via insertion of the basis representation for $\delta\rho^{\text{cpe}}(\mathbf{r})$, eq 11 is transformed into

$$E_{\text{cpe}}[\rho] = E[\rho^{\text{ref}} + \delta\rho^{\text{cpe}}] - E[\rho^{\text{ref}}] = E_{\text{cpe}}[\mathbf{q}, \mathbf{c}] \tag{13}$$

which leads to an algebraic set of equations of the following form:

$$E_{\text{cpe}}[\mathbf{q}, \mathbf{c}] = \mathbf{c}^T \cdot \mathbf{M} \cdot \mathbf{q} + \frac{1}{2} \mathbf{c}^T \cdot \mathbf{N} \cdot \mathbf{c} \tag{14}$$

where $\mathbf{q}$ denotes the vector of atomic Mulliken charges from DFTB3. In eq 14, the first and second functional derivatives appearing in eq 11 are approximated by Coulombic interactions between basis functions:

$$M_{ij} = f(R_{ij}) \iint \frac{\varphi_i^{\text{cpe}}(\mathbf{r})\, \varphi_j^{\text{dftb3}}(\mathbf{r}')}{|\mathbf{r} - \mathbf{r}'|}\, \mathrm{d}^3 r\, \mathrm{d}^3 r' \tag{15}$$

$$N_{ij} = \iint \frac{\varphi_i^{\text{cpe}}(\mathbf{r})\, \varphi_j^{\text{cpe}}(\mathbf{r}')}{|\mathbf{r} - \mathbf{r}'|}\, \mathrm{d}^3 r\, \mathrm{d}^3 r' \tag{16}$$

Here, Gaussian dipolar basis functions describe the CPE response density as

$$\varphi_i^{\text{cpe}}(\mathbf{r}) = -2\zeta(q_i)^2 \left(\frac{\zeta^2}{\pi}\right)^{3/2} (k - K_i) \mathrm{e}^{\zeta^2 |\mathbf{r} - \mathbf{R}_i|^2} \tag{17}$$

in which k is either x, y, or z and K_i is either X_i, Y_i, or Z_i, a component of the atomic position of atom i. The exponential factor, ζ, denotes an empirical parameter. To be able to account for the strong dependency of molecular polarizability as a function of the number of electrons in a system (i.e., its charge state), a monoexponential relation was assumed for ζ equal to the one proposed in the former work of Giese et al.[37] as

$$\zeta(q_i) = Z_i\, \mathrm{e}^{B_i q_i} \tag{18}$$

where the value of ζ depends exponentially on the partial charge q_i of atom i as derived from DFTB3. In contast to the CPE dipolar Gaussian basis, charge density fluctuations in DFTB3 are described by monopolar Slater functions as

$$\varphi^{\text{dftb3}}(\mathbf{r}) = \frac{\tau_i^3}{8\pi}\, \mathrm{e}^{-\tau_i |\mathbf{r} - \mathbf{R}_i|} \quad \text{with } \tau_i = \frac{16}{5}\left(U_i + \frac{\partial U_i}{\partial q_i} q_i\right) \tag{19}$$

It should be noted that the expression for τ is rather empirically chosen for the purpose of including charge dependency. As already mentioned in the Introduction, in the framework of these monopoles only radial but not angular dependent changes in the charge density can be captured.

The screening function, f, in eq 15, introduced earlier by Giese et al.,[37] has proven to be a useful empirical tool to capture the balancing effect of the kinetic energy that has been neglected by the Coulomb approximation of the first and second functional derivatives in eq 11. The screening function used here is

$$f(R_{ij}) = \begin{cases} 1, & \text{if } R_{ij} > R_u \\ 0, & \text{if } R_{ij} < R_l \\ 1 - 10x^3 + 15x^4 - 6x^5, & \text{otherwise} \end{cases} \tag{20}$$

where

$$R_u = R_{i,u} + R_{j,u} \tag{21}$$

$$R_l = R_{j,l} + R_{j,l} \tag{22}$$

Here, $R_{i,u}$ and $R_{i,l}$ are empirical parameters associated with atom i, which define interatomic distances where the screening function is turned on. The variable x is defined as

dx.doi.org/10.1021/jp306239c | J. Phys. Chem. A 2012, 116, 9131−9141

$$x = \frac{R_u - R_{ij}}{R_u - R_l} \tag{23}$$

The CPE response coefficients that minimize eq 14 are

$$\mathbf{c} = -\mathbf{N}^{-1}\cdot\mathbf{M}\cdot\mathbf{q} \tag{24}$$

Because of the alteration of atomic charges, q_i, as a function of the DFTB3 SCF cycle and since the CPE energy expression depends on these charges, the CPE solution must be entered back into the DFTB3 Hamilton matrix, $\mathbf{H}_{\mu\nu}$ (see Figure 1). Just as DFTB3 maps the density matrix into a basis of atomic charges, so too must the atom potentials be mapped into the Hamilton matrix.

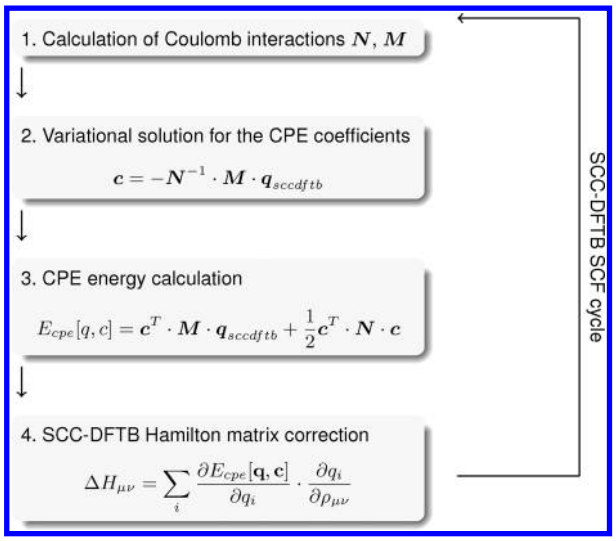

Figure 1. Schematic representation of the CPE framework as imbedded into DFTB3.

These atom potentials, p_i [i.e. the derivatives of the CPE energy (eq 14)], wrt the charges, q_i, can be written as

$$p_i = \frac{\partial E_{\mathrm{cpe}}[\mathbf{q},\mathbf{c}]}{\partial q_i} = \mathbf{c}\cdot\mathbf{M} + \mathbf{q}\cdot(\mathrm{d}\mathbf{M}/\mathrm{d}q_i)\cdot\mathbf{c} + \frac{1}{2}\mathbf{c}^T\cdot(\mathrm{d}\mathbf{N}/\mathrm{d}q_i)\cdot\mathbf{c} \tag{25}$$

Finally, the Hamilton matrix correction $\Delta\mathbf{H}_{\mu\nu}$ can be written as

$$\Delta\mathbf{H}_{\mu\nu} = \sum_i p_i \frac{\partial q_i}{\partial \rho_{\mu\nu}} \tag{26}$$

where $\rho_{\mu\nu}$ is the single-particle DFTB3 density matrix.

The major steps of the CPE procedure as implemented in DFTB3 are summarized schematically in Figure 1. From the set of coefficients, c_j, for the CPE basis functions and dipole moment of the standard DFTB3 reference method, a new molecular dipole moment μ_i^{cpe} can be defined as

$$\mu_i^{\mathrm{cpe}} = \mu_i^{\mathrm{dftb3}} + \sum_j^N c_j, \quad \text{with } i = x, y, z \tag{27}$$

In analogy to eq 6, the finite electric-field approach is used again for the evaluation of the polarizability tensor, $\boldsymbol{\alpha}$, utilizing the CPE-corrected dipole moment μ_i^{cpe} as

$$\boldsymbol{\alpha}_{ij}^{\mathrm{cpe}} = \left(\frac{\partial \mu_i^{\mathrm{cpe}}}{\partial F_j}\right) \quad \text{with } i, j = x, y, z \tag{28}$$

Raman Intensities. For the calculation of Raman spectra, the normal mode analysis (NMA) method as implemented in GAUSSIAN 03[44] was used to generate the reference data on the DFT level. With concern of SCC-DFTB, spectra were calculated from an inhouse NMA approach. At this point, we will just briefly present the equations for the calculation of Raman activities. For a comprehensive treatment of the Raman effect, please refer to the literature (e.g., Long[39]). By default, the Raman activity, A_k, for each individual normal mode of vibration, Q_k, in the system is evaluated via

$$A_k = \frac{1}{45}(45\bar{\alpha}_{\mathrm{iso}}{}^2 + 13\bar{\alpha}_{\mathrm{aniso}}{}^2) \tag{29}$$

where $\bar{\alpha}_{\mathrm{iso}}$ and $\bar{\alpha}_{\mathrm{aniso}}$ denote the normal coordinate derivatives of the two rotational invariants of the polarizability tensor, $\boldsymbol{\alpha}_{\mathrm{iso}}$ and $\boldsymbol{\alpha}_{\mathrm{aniso}}$, respectively. Those are calculated as

$$\bar{\alpha}_{\mathrm{iso}}{}^2 = \frac{1}{9}\left(\frac{\partial\alpha_{xx}}{\partial Q_k} + \frac{\partial\alpha_{yy}}{\partial Q_k} + \frac{\partial\alpha_{zz}}{\partial Q_k}\right)^2 \tag{30}$$

$$\bar{\alpha}_{\mathrm{aniso}}{}^2 = \frac{1}{2}\left[\left(\frac{\partial\alpha_{xx}}{\partial Q_k} - \frac{\partial\alpha_{yy}}{\partial Q_k}\right)^2 + \left(\frac{\partial\alpha_{xx}}{\partial Q_k} - \frac{\partial\alpha_{zz}}{\partial Q_k}\right)^2 + \left(\frac{\partial\alpha_{yy}}{\partial Q_k} - \frac{\partial\alpha_{zz}}{\partial Q_k}\right)^2 + 6\left(\left(\frac{\partial\alpha_{xy}}{\partial Q_k}\right)^2 + \left(\frac{\partial\alpha_{yz}}{\partial Q_k}\right)^2 + \left(\frac{\partial\alpha_{xz}}{\partial Q_k}\right)^2\right)\right] \tag{31}$$

Parametrization and Performance of DFTB3/CPE. For the CPE parametrization of DFTB3, the structures of 172 small organic molecules ranging from 3 to 14 atoms and containing elements H, S, N, O, S, and P were taken from the QCRNA[40] database along with their molecular properties of interest. Overall, the set contains 112 neutral, 37 monoanionic, and 23 monocationic model compounds for which dipole moments (using a 6-311G++(3df,2p) triple-ζ basis) and polarizabilities (using a 6-31G++(p,d) double-ζ basis) were generated with DFT together with Becke's B3LYP[21] exchange-corrrelation functional, as implemented in Gaussian 03.

For the current CPE implementation, overall, 24 empirical fit parameters (for H, S, N, O, S, and P) were required [i.e., two distance parameters, $R_{i,u}$ and $R_{i,l}$, for the switching function (eq 20) and two parameters, Z_i and B_i, for the CPE ζ-exponent (eq 18)]. The empirical parameters where chosen to minimize the discrepancy between the norm of molecular dipole moments, μ, and isotropic polarizabilities, α_{iso}, evaluated as

$$\mu = \sqrt{\mu_x^2 + \mu_y^2 + \mu_z^2} \tag{32}$$

$$\alpha_{\mathrm{iso}} = \frac{1}{3}(\alpha_{xx} + \alpha_{yy} + \alpha_{zz}) \tag{33}$$

from DFTB3 calculations with respect to target data from full density functional calculations. The merit function, Θ, to be minimized during the parametrization process can be written as

dx.doi.org/10.1021/jp306239c | J. Phys. Chem. A 2012, 116, 9131−9141

$$\Theta = \sum_{i}^{172} (\mu_i - \mu_{\mathrm{ref},i}) + \sum_{i}^{172} (\alpha_i^{\mathrm{iso}} - \alpha_{\mathrm{ref},i}^{\mathrm{iso}}) \quad (34)$$

RESULTS AND DISCUSSION

The optimized set of empirical parameters for the switching function, f, and Slater exponents, ζ, in the CPE basis functions are listed in Table 1.

Table 1. Optimized Set of Empirical CPE Fit Parameters for DFTB3

	Z (au)	B (au)	$R_{i,l}$ (au)	$R_{i,u}$ (au)
H	4.10743330	4.37992780	0.65017096	0.89976532
C	2.12941380	0.46271552	1.58230960	2.60816630
O	4.59123620	1.05271210	4.14445140	4.50938330
N	2.58954660	0.50147210	2.99983790	3.12407570
S	2.26117890	0.74985889	3.40497140	624.334400
P	36.9483900	105.240460	74.7108830	1998.27850

In Figures 2−4, the performance of DFTB3/CPE for the calculation of the mean molecular polarizability is shown and compared with the reference data from the DFT and results from the standard DFTB3. Generally, the results show several clear tendencies. Most striking is the systematic underestimation of molecular polarizability from standard DFTB3 compared to DFT reference data for neutral, cationic, and monoanionic compounds, an observation in line with previous studies.[38]

Furthermore, an increasing deviation of the DFTB3 results from the reference with an increasing number of electrons (charge state) in the system can be observed. The error in mean polarizability (see Figures 2−4) approximately doubles when going from cationic (7.036 au error) to neutral (16.971 au error) compounds and again when going to anionic (34.358 au error) molecules. Apart from that, the deviation between the DFTB3 results and the DFT reference also increases with increasing absolute polarizability of the system, illustrated by increasing differences from the left to right side of the graphs in Figures 2−4. The results from the parametrized DFTB3/CPE approach (also shown in Figures 2−4) reveal a significant improvement for the calculated isotropic polarizabilities. Most notably, an almost equally good agreement is achieved along the different charge states of molecules, due to the fact that the current CPE implementation accounts for charge dependency of molecular polarization.

To emphasize the progress the current CPE extension delivers in this respect, the molecular polarizability of a glycine residue as a function of its charge state is presented in Table 2. As shown in the table, DFTB3 not only underestimates values for the polarizabilities itself but also, more severely, shows the wrong tendency, a decreasing polarizability with an increasing number of electrons in the system. For both of these errors, the currently implemented DFTB3/CPE approach denotes a dramatic improvement. Aside from polarizability calculations on single molecules, we have also tested the CPE parameters on a water dimer to figure out its performance for molecular complexes. In Figure 5, the polarizability of the dimer is plotted against the intermolecular distance of the monomers. As observed for single molecules, the polarizability of the dimer is underestimated by DFTB3 by a factor of ∼2.5 compared to full DFT over the entire range of distances. This deviation to the reference data is again significantly reduced within the DFTB3/CPE approach. To analyze the inherent problems in electronic polarizability calculations of DFTB3 in more detail, the complete tensors of two molecules, water and benzene, are shown in Figure 6. For water, only the diagonal elements are non-zero from both the reference data (DFT) and DFTB3. Although all three diagonal elements from DFTB3 are smaller compared to those from the DFT, the deviation is especially large for the *xx*-component of the tensor where DFTB3 predicts zero polarizability out of plane. As mentioned in

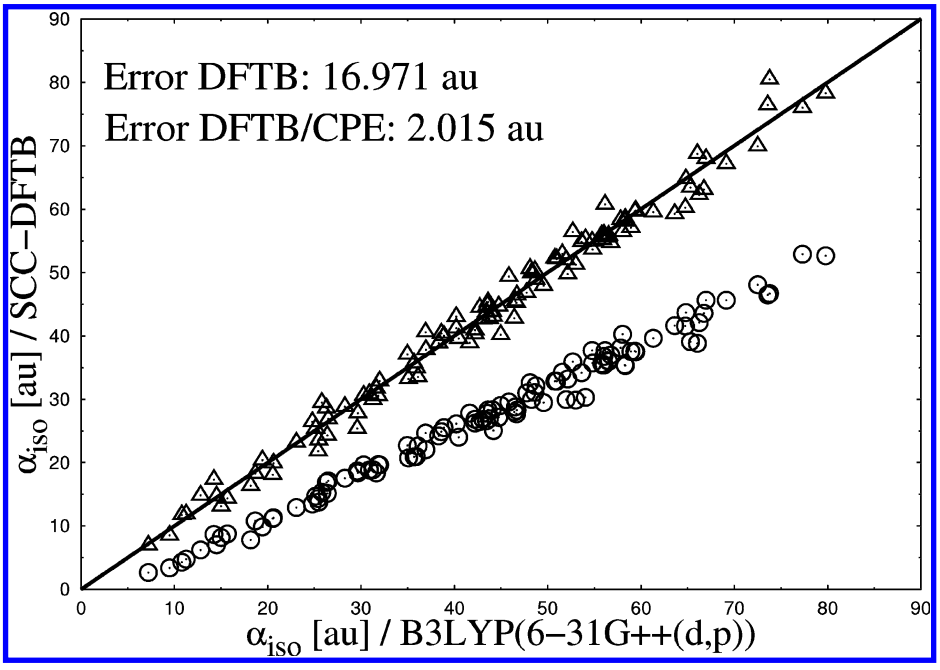

Figure 2. Calculated isotropic molecular polarizabilities for a set of 112 neutral organic molecules. Results from the DFTB3 (⊙) and DFTB3/CPE (△) calculations are compared with those from the DFTB/B3LYP reference data (diagonal line).

dx.doi.org/10.1021/jp306239c | J. Phys. Chem. A 2012, 116, 9131−9141

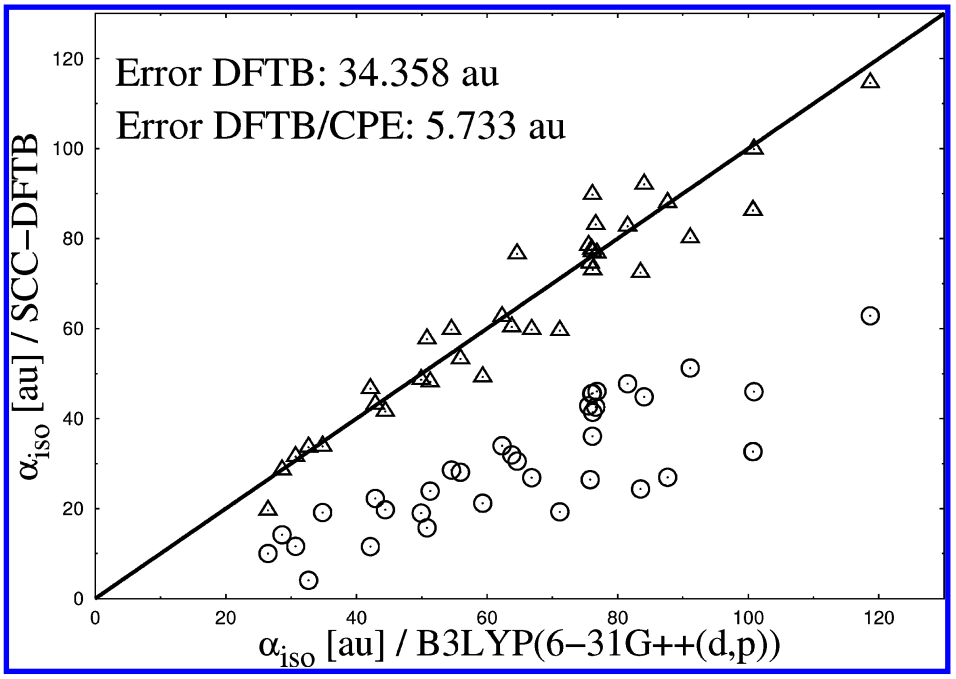

Figure 3. Calculated isotropic molecular polarizabilities for a set of 37 monoanionic organic molecules. Results from the DFTB3 (⊙) and DFTB3/CPE (△) calculations are compared with those from the DFTB/B3LYP reference data (diagonal line).

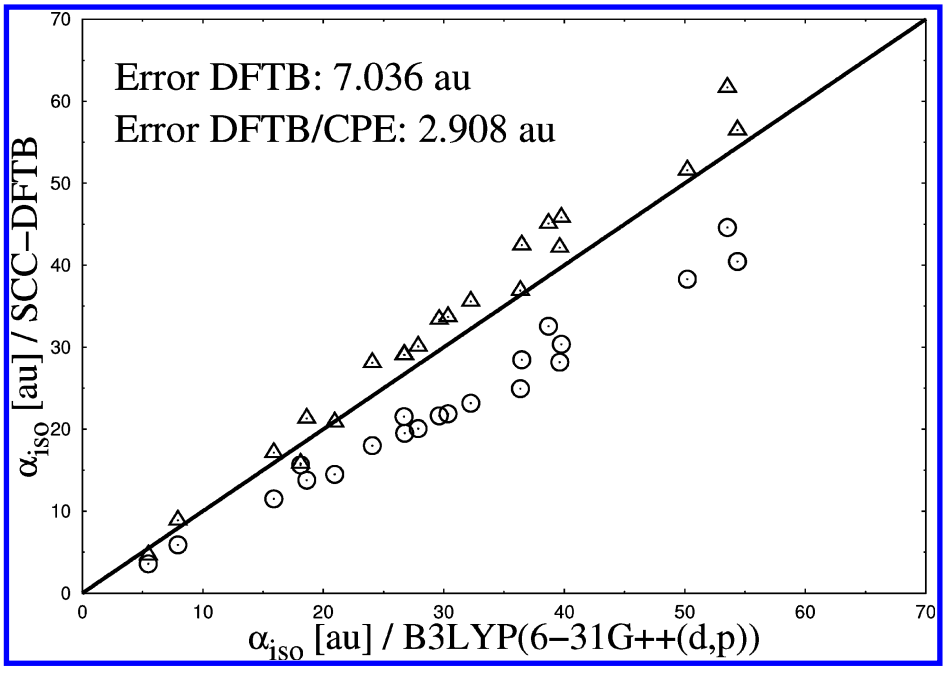

Figure 4. Calculated isotropic molecular polarizabilities for a set of 23 monocationic organic molecules. Results from the DFTB3 (⊙) and DFTB3/CPE (△) calculations are compared with those from the DFTB/B3LYP reference data (diagonal line).

Table 2. Comparison of Calculated Mean Molecular Polarizabilities[a] as a Function of Charge State for the Amino Acid Glycine

charge state	DFT/B3LYP	DFTB3	DFTB3/CPE
+1	36.4	24.9	36.9
0	40.5	24.0	39.6
−1	51.3	23.9	48.1

[a]Values are given in au.

Theoretical Approach, the monopole Slater representation of charge fluctuations (see eq 18) is insufficient to describe polarization out of a molecular plane. This systematic shortcoming is largely removed by the current CPE extension, as shown in Figure 6. From the DFTB3/CPE approach, all diagonal elements are in closer agreement with the DFT reference. The same observation holds for benzene concerning the diagonal tensor elements. Here again, very little out-of-plane polarizability (*xx*-component) is observed from the DFTB3 calculations, a situation significantly improved with the DFTB3/CPE approach. The off-diagonal elements (*xz*/*zx*-

dx.doi.org/10.1021/jp306239c | J. Phys. Chem. A 2012, 116, 9131−9141

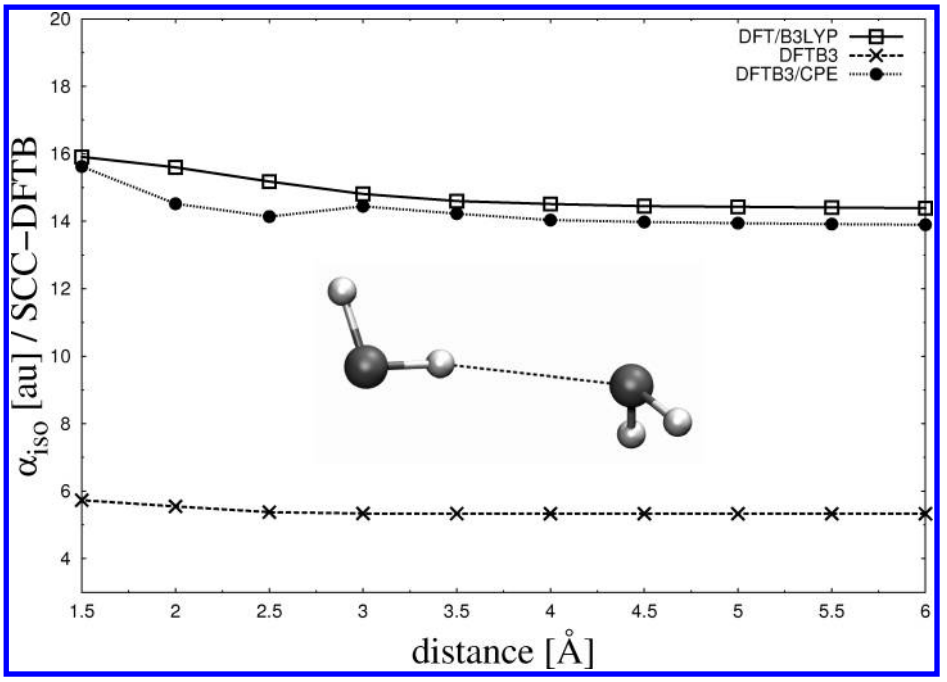

Figure 5. Comparison of calculated isotropic molecular polarizabilities as a function of intermolecular distance for a water dimer.

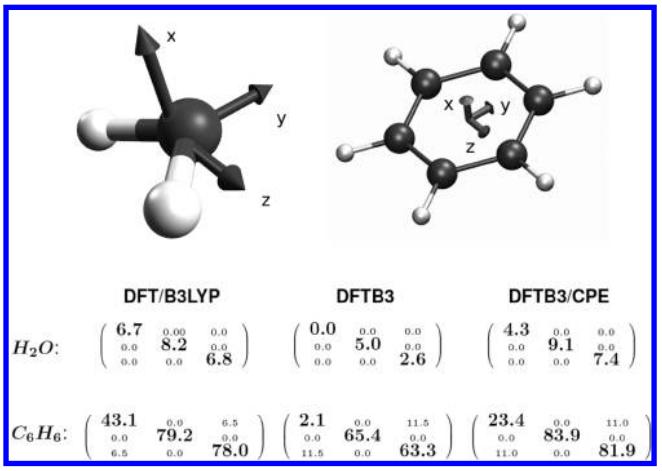

Figure 6. Comparison of polarizability tensors for water and benzene (both oriented in the *yz*-plane) as calculated from the DFT/B3LYP and DFTB3 levels of theory. Diagonal elements are emphasized.

components) for benzene, however, show a clear overestimation from the DFTB3 calculations compared to the reference by a factor of ∼2, which also holds for the DFTB3/CPE approach. This observation of overestimation of off-diagonal elements is a tendency also true for the majority of test molecules and is shown in Figure 7. Here, the anisotropic component of the polarizability tensor

$$\alpha_{\text{aniso}} = \frac{1}{2}[(\alpha_{xx} - \alpha_{yy}) + (\alpha_{yy} - \alpha_{zz}) + (\alpha_{zz} - \alpha_{xx}) + 6(\alpha_{xy} - \alpha_{yz} + \alpha_{yz})] \tag{35}$$

is plotted. Since all elements of the tensor appear in α_{aniso}, not just diagonal ones as in α_{iso} and because of the first three different terms, which are more prone to error, α_{aniso} is harder to evaluate accurately. The plot shows three different graphs which all show the same basic pattern (i.e., a clear overestimation of the anisotropic component compared to full DFT over the entire range of 112 neutral test molecules). From the deviations of anisotropic polarizability given in Figure 7, it can also be seen that the DFTB3/CPE/iso-fit (10.732 au) does not give any improvement over the standard DFTB3 method (9.091 au). Here, the extension "iso-fit" is used to clarify that the CPE parameters have been optimized for only the isotropic components (α_{iso}) of the tensor so far. Therefore, a reparametrization has been performed, where the anisotropic components were also included in the merit function Θ as

$$\Theta = \sum_{i}^{172} (\mu_i - \mu_{\text{ref},i}) + \sum_{i}^{172} (\alpha_i^{\text{iso}} - \alpha_{\text{ref},i}^{\text{iso}}) + \sum_{i}^{172} (\alpha_i^{\text{aniso}} - \alpha_{\text{ref},i}^{\text{aniso}}) \tag{36}$$

The results from the reparametrization, also presented in Figure 7 and denoted with DFTB3/CPE/iso+aniso fit, show no notable improvement for α_{aniso}. With the current CPE implementation, no parameter set was found to reproduce equally well both rotational invariants, α_{iso} and α_{aniso}, of the polarzability tensor.

Raman Intensities from DFTB3/CPE. So far, we've focused on absolute electronic polarizabilities. The ability to accurately describe polarizability changes as a function of normal mode vibrations, however, opens the way to the prediction of Raman vibrational spectra. As already discussed in the theory section, Raman intensities (or activities) are connected to first-order polarizability derivatives with respect to normal mode vibrations, Q_k. As a first test of how CPE performs for those derivatives, we replaced them by finite differences as

$$A_k \propto \left(\frac{\partial \alpha}{\partial Q_k}\right)^2 \approx \left(\frac{\Delta \alpha}{\Delta Q_k}\right)^2 \tag{37}$$

For a subset of the test molecules, we took the optimized DFT structure and its polarizability as a reference (α_{opt}), which

dx.doi.org/10.1021/jp306239c | J. Phys. Chem. A 2012, 116, 9131−9141

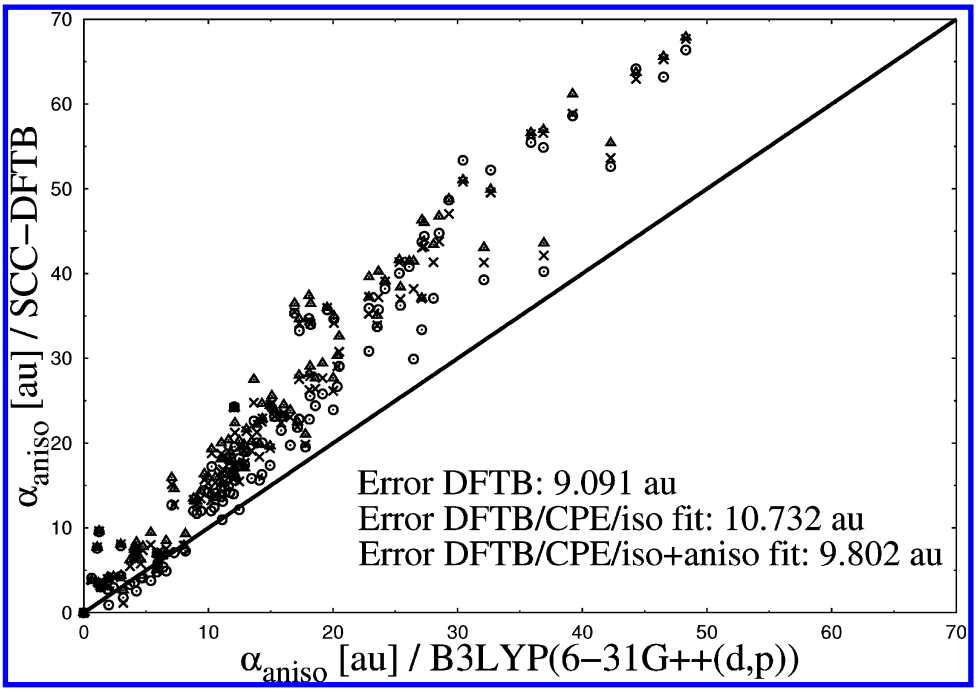

Figure 7. Calculated anisotropic molecular polarizabilities for a set of 112 neutral organic molecules. Results from the DFTB3 (⊙), the DFTB3/CPE/iso (△) and the DFTB/CPE/aniso (×) calculations are compared with those from the DFTB/B3LYP reference data (diagonal line).

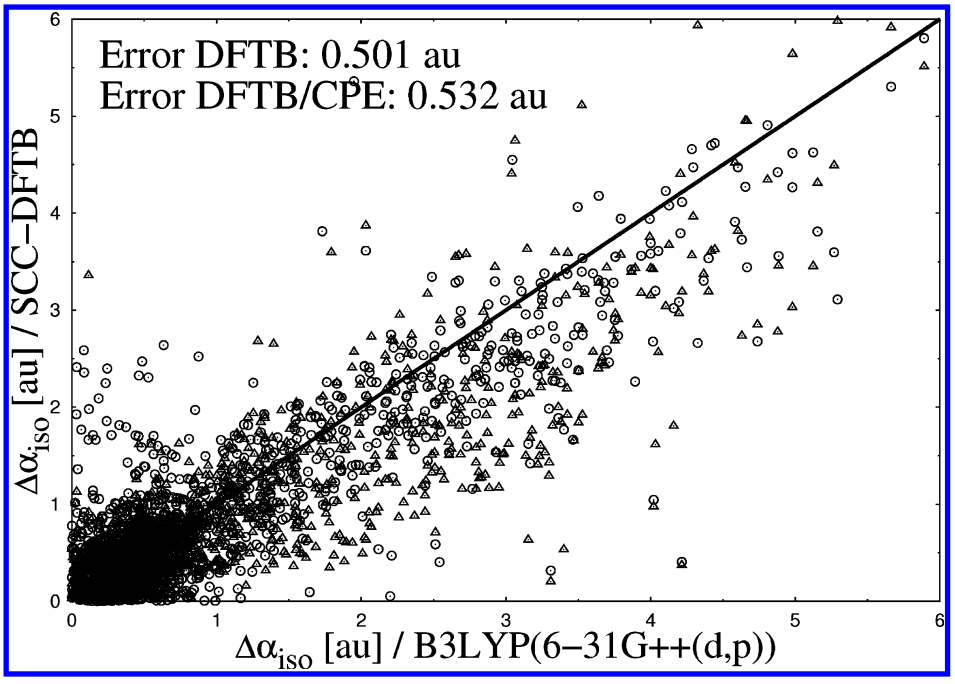

Figure 8. Calculated differences of isotropic molecular polarizabilities for a subset of test molecules. Results from the DFTB3 (⊙) and DFTB3/CPE (△) calculations are compared with those from the DFTB/B3LYP reference data (diagonal line).

was subsequently subtracted by the resulting polarizability from the molecule in a distorted structure (α_{dist}) along a certain normal mode of vibration, so that $\Delta\alpha$ in eq 37 becomes

$$\Delta\alpha_{iso} = \alpha_{iso}^{opt} - \alpha_{iso}^{dist} \quad (38)$$

$$\Delta\alpha_{aniso} = \alpha_{aniso}^{opt} - \alpha_{aniso}^{dist} \quad (39)$$

The same molecular structures were used for calculations with DFTB3 for comparison. In Figures 8 and 9, the results are shown for $\Delta\alpha_{iso}$ and $\Delta\alpha_{aniso}$ for a set of overall 1847 normal modes of vibration. Via comparison of the scatter plots from both figures, the same tendency appears for the polarizability differences as for the absolute values. While most of the data points for $\Delta\alpha_{iso}$ from DFTB3 are below the reference diagonal line from the full DFT, meaning an underestimation of polarizability change, the data points of $\Delta\alpha_{iso}$ spread more homogeneously around the reference with little tendency of overestimation. As pointed out in Figures 8 and 9, the average deviation of DFTB3 from the reference is twice as large for $\Delta\alpha_{iso}$ (0.501 au) compared to $\Delta\alpha_{aniso}$ (1.005 au), reflecting that

dx.doi.org/10.1021/jp306239c | J. Phys. Chem. A 2012, 116, 9131−9141

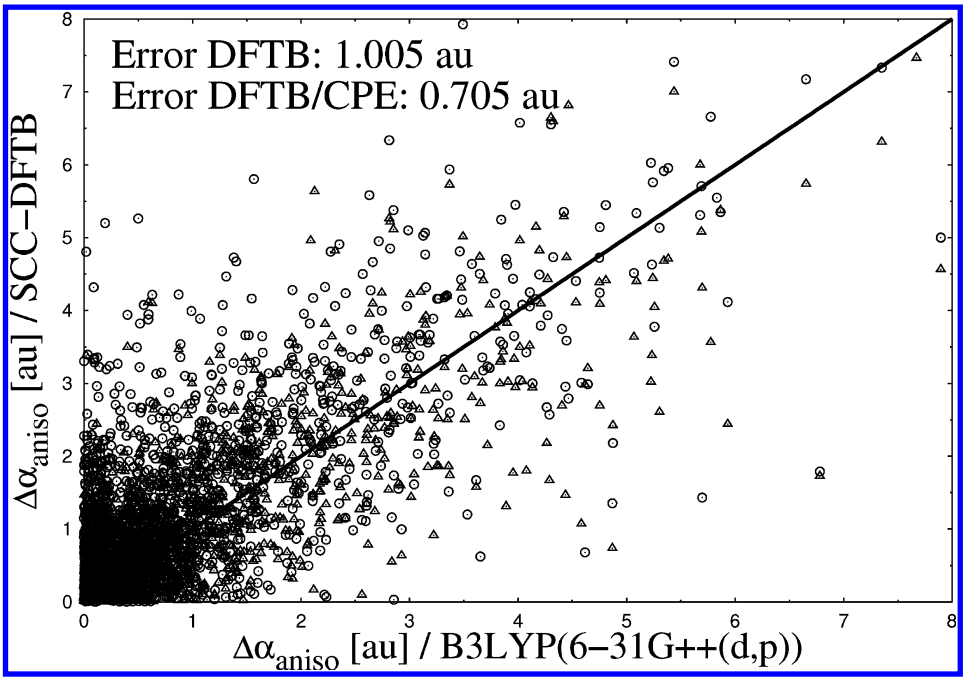

Figure 9. Calculated differences of isotropic molecular polarizabilities for a subset of test molecules. Results from the DFTB3 (⊙) and DFTB3/CPE (△) calculations are compared with those from the DFTB/B3LYP reference data (diagonal line).

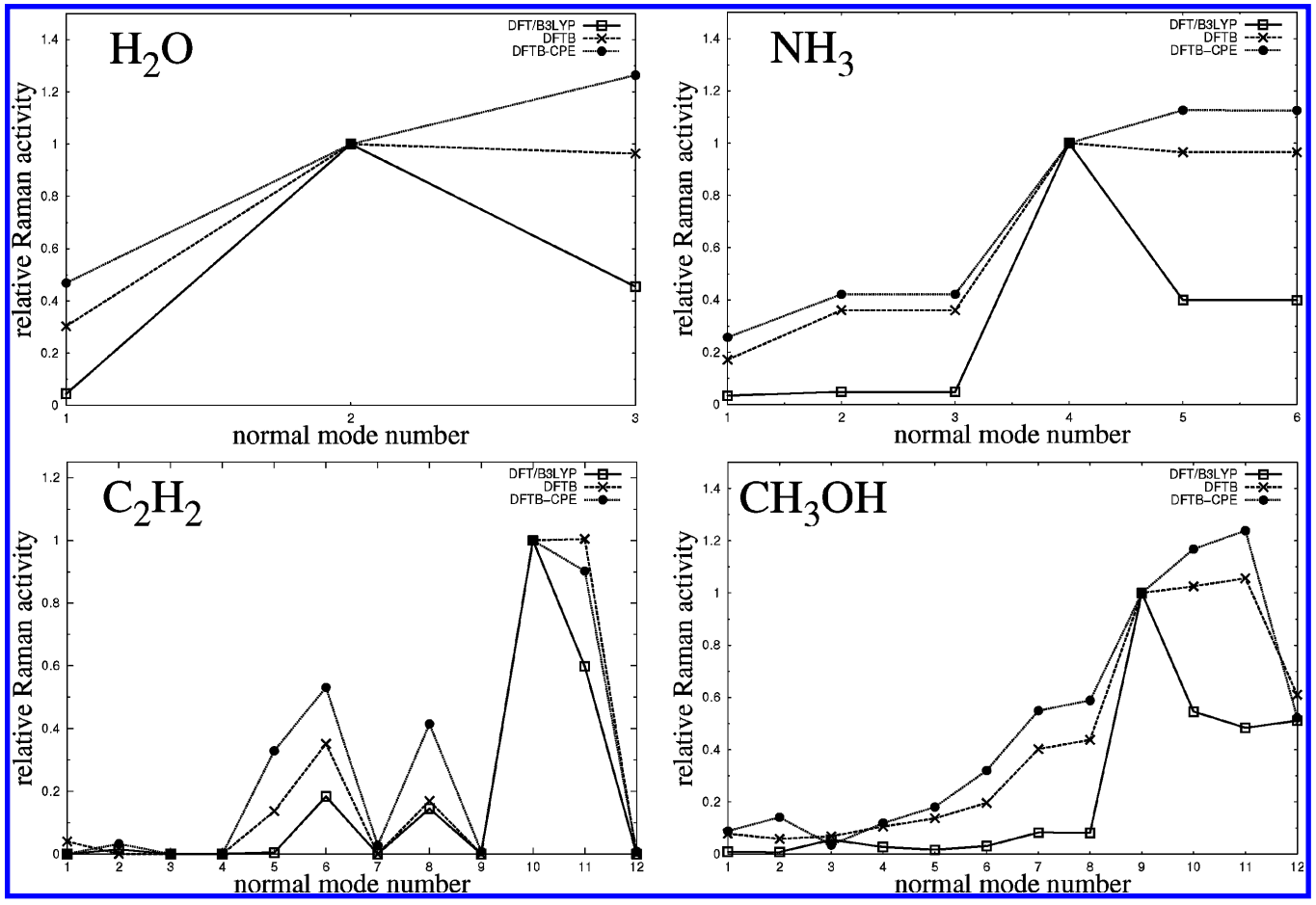

Figure 10. Comparison of calculated Raman activities plotted against the normal mode number, for four small-sized molecules and different levels of theory. Here, the normal mode number denotes a vibrational mode being of the same character for both levels of theory (DFT and DFTB3), increasing from low to high energies (vibrational frequencies). All graphs for a specfic molecule are normalized to unity with respect to the activity of a certain vibrational mode. In particular, mode 2 for H_2O, mode 4 for NH_3, mode 10 for C_2H_2, and mode number 9 for CH_3OH.

dx.doi.org/10.1021/jp306239c | J. Phys. Chem. A 2012, 116, 9131–9141

the latter is more difficult to evaluate accurately. In this respect, it is remarkable that with the CPE extension of DFTB3 the average deviation of $\Delta\alpha_{aniso}$ from the reference could be reduced by ~30% (1.05 vs 0.705 au), while CPE has no notable effect on $\Delta\alpha_{iso}$ (0.501 vs 0.532 au).

As a final test in which we go from finite differences for electronic polarizabilities to first-order derivatives, Raman activities were calculated for a small subset of test molecules. In Figure 10, the results are shown for four molecules. We restricted the analysis to very small molecules to achieve a low density of states (DOS) in the interesting mid-infrared region, in order to keep the assignment of vibrational modes simple. For each molecule, three graphs (DFT vs DFTB3 vs DFTB3/CPE) are presented, where Raman activities are plotted against the vibrational mode number. For better comparison of the relative activities (we are not interested in absolute activities), all the graphs are normalized to unity against the mode with the highest activity from the DFT reference. From the graphs in Figure 10, two tendencies can be observed. For all molecules, the relative activities are systematically overestimated by DFTB3 compared to those of the reference over the entire spectral range. This effect is even more pronounced for DFTB3/CPE, which leads to a stronger overestimation for the activities. Further, modes in the high-frequency region (frequency increases with mode number) tend to be more greatly overestimated as modes in the region of lower frequencies, which is especially true for H_2O, NH_3, and CH_3OH.

SUMMARY AND CONCLUSIONS

In the present work, we successfully implemented and parametrized the chemical-potential equalization method (CPE) into the DFTB3 program, in order to calculate accurate electronic polarizabilities. The improvements of DFTB3 over DFTB2 and DFTB for molecular properties have been discussed in detail recently.[35] The main improvements found for DFTB3 are basically related to a better description of charged molecules, particularly relevant for this work.

We were encouraged to add CPE to DFTB3 because of significant improvements that York and Giese achieved with an MNDO/CPE code for polarizabilitiy calculations when compared to standard MNDO. As for semiempirical methods in general, SCC-DFTB also works with a minimal atomic orbital basis, which is critical since the accuracy of electronic polarizability depends strongly on the size of the ao-basis. In the current CPE formalism response, density is added to the system without increasing the ao-basis, which keeps the computational cost fairly low. Aside from the minimal ao-basis, the restriction of the second-order terms to monopole contributions may also severely limit the SCC-DFTB's ability to describe density response properties. This is also confirmed by further results presented in the Supporting Information where the performance of CPE implemented into DFTB2 is shown. Since both DFTB2 and DFTB3 are characterized by the same approximations (i.e., minimal basis and monopole representation of charge fluctuations), the errors for polarizabilities in the standard implementations and the improvements when CPE is employed are very similar (see Supporting Information). In fact, DFTB3 does not perform notably better in polarizability calculations of neutral molecules than DFTB2 because of the same basic limitations.

For charged molecules, however, there is a drastic improvement due to the charge-dependent exponent of the CPE basis functions. Note that this can also be added to the DFTB2 formalism in an ad hoc fashion, but its formal justification comes from the DFTB3 extension, where a charge-dependent Hubbard is derived from the third-order expansion of the DFT total energy. Therefore, a formally consistent application of the charge-dependent CPE is possible only at the DFTB3 level, leading to a significantly improved description of charged molecules[35] and their polarizabilities, as shown in this work.

With an overall number of 24 optimized empirical parameters for elements H, S, N, O, S, and P, the DFTB3/CPE approach has been shown to correct for these shortcomings of the original SCC-DTB to give very accurate mean (isotropic) polarizabilities, in comparison with the full DFT reference data, for a large set of small- to medium-sized organic molecules. This accuracy, however, comes at a considerable lower computational cost, with SCC-DFTB being 3 orders of magnitude faster than DFT. Another shortcoming of SCC-DFTB, the inability to predict the strong charge dependence of electronic polarizability, could also be removed by the present DFTB3/CPE approach. While DFTB3/CPE can be successfully applied for the calculation of isotropic polarizabilities (average of diagonal tensor elements) alone, the entire polarizability tensor remains a challenging task. It seems that off-diagonal elements tend to be overestimated while diagonal elements are underestimated by SCC-DFTB. In fact, no single parameter set could be found within the current framework of DFTB3/CPE to predict both rotational invariants of the polarizability tensor accurately.

The observation that the CPE correction largely improves the isotropic polarizability is consistent with previous observations and primarily due to the fact that the CPE dipole functions have an isotropic self-energy; that is, the diagonal elements of the **N**-matrix are the same for the *x*-, *y*-, and *z*-directions. In this way, the model itself is a superposition of loosely coupled isotropic dipolar response functions and, therefore, largely isotropic.

Aside from the absolute values of polarizability, their changes along vibrational modes were also investigated to estimate the ability of the DFTB3/CPE approach for Raman activity calculations. In this respect, only changes in anisotropic polarizability were improved from DFTB3/CPE compared to the full DFT, which remains rather questionable to us since the anisotropic component is the more complex value compared to the isotropic one.

As a matter of fact, the current implementation of DFTB3/CPE also cannot contribute to the improvement of Raman activities (i.e., polarizability derivatives); instead the agreement with the reference DFT is worse compared to plain DFTB3. Here, the damping function in the first Coulomb integral expression may be responsible for that. Since the function screens out the Coulombic interactions for atoms which are close in distance and because molecular vibrations elongate bonds by approximately 0.1 Å, normal mode vibrations may cause too little structural and, therefore, polarizability changes to be captured by the current CPE implementation.

As future work, a modified CPE approach capable of "fine-tuning" the polarizability as a function of bond length could be helpful for parametrically reproducing Raman spectra.

ASSOCIATED CONTENT

Supporting Information

A brief description of the implementation, parametrization, and performance of the current CPE formalism in a charge-

dependent and charge-independent framework into the second-order SCC-DFTB code is given. This material is available free of charge via the Internet at http://pubs.acs.org.

AUTHOR INFORMATION

Corresponding Author

*D.M.Y.: e-mail, york@biomaps.rutgers.edu. M.E.: e-mail, marcus.elstner@kit.edu.

Notes

The authors declare no competing financial interest.

ACKNOWLEDGMENTS

The authors D.M.Y. and T.J.G. are grateful for financial support provided by the National Institutes of Health (GM084149). Financial support by the DFG project EL 206/11-1 is acknowledged.

REFERENCES

(1) Hückel, E. *Z. Phys.* **1933**, *83*, 632.
(2) Pariser, R. *J. Chem. Phys.* **1953**, *21*, 767.
(3) Pople, J. A.; Segal, G. A. *J. Chem. Phys.* **1966**, *44*, 3289.
(4) Dewar, M. J. S.; Thiel, W. *Theor. Chim. Acta* **1977**, *46*, 89.
(5) Clark, T. *THEOCHEM* **2000**, *530*, 1.
(6) Dewar, M. J. S.; Thiel, W. *J. Am. Chem. Soc.* **1977**, *99*, 4899.
(7) Dewar, M. J. S.; Zoebisch, E. G.; Healy, E. F.; Stewart, J. J. P. *J. Am. Chem. Soc.* **1985**, *107*, 3902.
(8) Stewart, J. J. P. *J. Comput. Chem.* **1989**, *10*, 209.
(9) Kolb, M.; Thiel, W. *J. Comput. Chem.* **1993**, *14*, 775.
(10) Thiel, W.; Voityuk, A. A. *Theor. Chim. Acta* **1992**, *81*, 391.
(11) Winget, P.; Thompson, J. D.; Xidos, J. D.; Cramer, C. J.; Truhlar, D. G. *J. Phys. Chem. A* **2002**, *106*, 10707.
(12) Burstein, K. Y.; Isaev, A. N. *Theor. Chim. Acta* **1984**, *64*, 397.
(13) Zerner, M. C.; Lipkowitz, K. B.; Boyd, D. B. *Semiempirical Molecular Orbital Methods, Reviews in Computational Chemistry*; VCH: New York, 1991; Vol. 2, p 45. (ZINDO actually does INDO/S calculations)
(14) Rinaldi, D.; Rivail, J. *Theor. Chim. Acta* **1974**, *32*, 57.
(15) Rinaldi, D.; Rivail, J. *Theor. Chim. Acta* **1974**, *32*, 243.
(16) Rivail, J. L.; Cartier, A. *Mol. Phys.* **1978**, *36*, 1085.
(17) Schürer, G.; Gedeck, P.; Gottschalk, M.; Clark, T. *Int. J. Quantum Chem.* **1999**, *75*, 17.
(18) Martin, B.; Gedeck, P.; Clark, T. *Int. J. Quantum Chem.* **2000**, *77*, 473.
(19) Hohenberg, P.; Kohn, W. *Phys. Rev.* **1964**, *136*, B864.
(20) Kohn, W.; Sham, L. J.; et al. *Phys. Rev.* **1965**, *140*, A1133.
(21) Becke, A. D. *Phys. Rev. A: At., Mol., Opt. Phys.* **1988**, *38*, 3098.
(22) Perdew, J. P.; Burke, K.; Ernzerhof, M. *Phys. Rev. Lett.* **1996**, *77*, 3865.
(23) Porezag, D.; Frauenheim, T.; Köhler, T.; Seifert, G.; Kaschner, G. *Phys. Rev. B: Condens. Matter Mater. Phys.* **1995**, *51*, 12947.
(24) Elstner, M.; Porezag, D.; Jungnickel, G.; Elsner, J.; Haugk, M.; Frauenheim, T.; Suhai, S.; Seifert, G. *Phys. Rev. B: Condens. Matter Mater. Phys.* **1998**, *58*, 7260.
(25) Sanderson, R. T. *Science* **1951**, *114*, 670.
(26) Gasteiger, J.; Marsili, M. *Tetrahedron* **1980**, *36*, 3219.
(27) Hinze, J.; Jaff, H. H. *J. Am. Chem. Soc.* **1962**, *84*, 540.
(28) Halls, M. D.; Schlegel, H. B. *J. Chem. Phys.* **1999**, *111*, 8819.
(29) Elstner, M. Ph.D. Thesis, University of Paderborn, Paderborn, Germany, 1998.
(30) Yang, Y.; Yu, H.; York, D.; Cui, Q.; Elstner, M. *J. Phys. Chem. A* **2007**, *111*, 10861.
(31) Elstner, M. *J. Phys. Chem. A* **2007**, *111*, 5614.
(32) Gaus, M.; Chou, C.-P.; Witek, H.; Elstner, M. *J. Phys. Chem. A* **2009**, *113*, 11866.
(33) Giese, T. J.; York, D. M. *Theor. Chem. Acc.* **2012**, *131*, 1145.
(34) Seifert, G. *J. Phys. Chem. A* **2007**, *111*, 5609.
(35) Gaus, M.; Qiang, C.; Elstner, M. *J. Chem. Theory Comput.* **2011**, *7*, 931.
(36) York, D. M.; Yang, W. *J. Chem. Phys.* **1996**, *104*, 159.
(37) Giese, T. J.; York, D. M. *J. Chem. Phys.* **2005**, *123*, 164108.
(38) Giese, T. J.; York, D. M. *J. Chem. Phys.* **2007**, *127*, 194101.
(39) Long, D. A. *The Raman Effect: A Unified Treatment of the Theory of Raman Scattering by Molecules*; John Wiley & Sons, Ltd.: Chichester, West Sussex, England, 2002.
(40) Giese, T. J.; Gregersen, B. A.; Liu, Y.; Nam, K.; Mayaan, E.; Moser, A.; Range, K.; Faza, O. N.; Lopez, C. S.; de Lera, A. R.; Schaftenaar, G.; Lopez, X.; Lee, T.; Karypis, G.; York, D. M. *J. Mol. Graphics Modell.* **2006**, *25*, 423.
(41) Parkinson, W. A.; Zerner, M. C. *J. Chem. Phys.* **1991**, *94*, 478.
(42) Dewar, M.; Yamaguchi, Y.; Suck, S. *Chem. Phys. Lett.* **1974**, *59*, 541.
(43) Matsuzawa, N.; Dixon, D. A. *J. Phys. Chem.* **1992**, *96*, 6232.
(44) Frisch, M. J.; Trucks, G. W.; Schlegel, H. B.; Scuseria, G. E.; Robb, M. A.; Cheeseman, J. R.; Montgomery, J. A., Jr.; Vreven, T.; Kudin, K. N.; Burant, J. C.; Millam, J. M.; Iyengar, S. S.; Tomasi, J.; Barone, V.; Mennucci, B.; Cossi, M.; Scalmani, G.; Rega, N.; Petersson, G. A.; Nakatsuji, H.; Hada, M.; Ehara, M.; Toyota, K.; Fukuda, R.; Hasegawa, J.; Ishida, M.; Nakajima, T.; Honda, Y.; Kitao, O.; Nakai, H.; Klene, M.; Li, X.; Knox, J. E.; Hratchian, H. P.; Cross, J. B.; Bakken, V.; Adamo, C.; Jaramillo, J.; Gomperts, R.; Stratmann, R. E.; Yazyev, O.; Austin, A. J.; Cammi, R.; Pomelli, C.; Ochterski, J. W.; Ayala, P. Y.; Morokuma, K.; Voth, G. A.; Salvador, P.; Dannenberg, J. J.; Zakrzewski, V. G.; Dapprich, S.; Daniels, A. D.; Strain, M. C.; Farkas, O.; Malick, D. K.; Rabuck, A. D.; Raghavachari, K.; Foresman, J. B.; Ortiz, J. V.; Cui, Q.; Baboul, A. G.; Cliffordzzz, S.; Cioslowski, J.; Stefanov, B. B.; Liu, G.; Liashenko, A.; Piskorz, P.; Komaromi, I.; Martin, R. L.; Fox, D. J.; Keith, T.; Al-Laham, M. A.; Peng, C. Y.; Nanayakkara, A.; Challacombe, M.; Gill, P. M. W.; Johnson, B.; Chen, W.; Wong, M. W. *Gaussian 03*, revision C02; Gaussian Inc.: Wallingford, CT, 2004.